HHS Public Access

Author manuscript

ACS Sens. Author manuscript; available in PMC 2020 January 02.

Published in final edited form as:

ACS Sens. 2019 October 25; 4(10): 2819–2824. doi:10.1021/acssensors.9b01532.

Chemiresistive Carbon Nanotube Sensors for *N*-nitrosodialkylamines

Maggie He[†], **Robert G. Croy**[†,‡], **John M. Essigmann**[†,‡], **Timothy M. Swager**[*,†]

[†]Department of Chemistry, Massachusetts Institute of Technology, 77 Massachusetts Avenue, Cambridge, Massachusetts 02139, United States

[‡]Departments of Biological Engineering and Center for Environmental Health Sciences, Massachusetts Institute of Technology, 77 Massachusetts Avenue, Cambridge, Massachusetts 02139, United States

Abstract

N-nitrosamines are environmental genotoxicants that are widely encountered in air, water, and food. Contamination of indoor and outdoor air with *N*-nitrosamines has been reported on many occasions. Conventional detection of airborne *N*-nitrosamines requires sophisticated instrumentation, field sampling, and laboratory analysis. Herein, we report ultra-sensitive carbon nanotube based chemiresistive sensors utilizing a Cobalt (III) tetraphenylporphyrin selector element for the detection of *N*-nitrosamines. Concentrations as low as 1 part per billion (ppb), of *N*-nitrosodimethylamine (NDMA), *N*-nitrosodiethylamine (NDEA) and *N*-nitrosodibutylamine (NDBA) were detected. We also demonstrate the integration of these sensors with a field deployable sensing node wherein the sensor response can be read online remotely.

Keywords

carbon nanotubes; chemiresistive; sensors; N-nitrosamines; N-nitrosodimethylamine; N-nitrosodiethylamine; N-nitrosodibutylamine

N-Nitrosamines are toxic compounds of high health concern that contaminate the environment. These compounds undergo reactions to produce reactive species that alkylate and damage DNA.[1] The American Conference of Governmental Industrial Hygienists has classified *N*-nitrosodimethylamine (NDMA) as an animal carcinogen (Group A3) and the Environmental Protection Agency has classified NDMA as a probable human carcinogen (Group B2).[2] Contamination by *N*-nitrosamines has been found in air, water, soil, food products, and manufactured goods. *N*-Nitrosamines are produced uninten- tionally through

[*]**Corresponding Author:** tswager@mit.edu.

Supporting Information

Supporting Information Available: The following files are available free of charge.

Supporting Information (PDF). General information, synthesis of porphyrins and functionalized CNTs, sensor fabrication, sensing setup, sensor responses in N_2 and in air, response of CNTs without selectors to NDMA, NMR spectra of H_2tpp, [Co(tpp)] and [Co(tpp)]ClO_4, binding experiments, device optimization, sensing under controlled humidity, detection of NDEA and NDBA, sensing setup with commercial sensing node, reversibility of sensors.

The authors declare no competing financial interest.

reactions of alkylamines with nitrogen oxides (NO, NO_2, N_2O_4, N_2O_3), nitrous acids, or nitrite salts, which can be found in various industrial processes, and are by- products from rubber manufacturing, leather tanning, pesticide production, dye synthesis, explosive/ propellant production, carbon capture,[3,4] and food processing.[5] *N*-Nitrosamines are also commonly found in environmental tobacco smoke.[6] NDMA can be further produced during chlorination of water[7] and has been found in beer[8] and cosmetics.[9]

Contamination of indoor and outdoor air with *N*-nitros- amines is a health concern for tobacco smokers, people living in urban areas, and workers in the rubber industry. High concentrations of NDMA were found in air close to industrial plants in Baltimore, Belle, and New York City in the 1970s.[10] Particularly in rubber and tire production, extremely high N-nitrosamine concentrations between 0.1 and 380 μg/m^3 (1 μg/m^3 NDMA = 3 ppb NDMA) were found in 19 factories in Germany from 1979 to 1983.[11] Concentrations as high as 99.9 μg/m^3 were found in 24 French factories from 1992 to 1995.[12] *N*-Nitrosomorpholine (NMOR) concentrations up to 27 μg/m^3 were found in Ohio rubber industry factories in 1978.[13] According to a 1990 Occupational Safety and Health Administration (OSHA) publication in the Safety and Health Information Bulletins, seven rubber manufacturing plants in the United States were contaminated with *N*-nitrosamines, including *N*-nitrosodiethylamine (NDEA), NDMA, NMOR, *N*-nitrosodiphenylamine, and *N*-nitrosopyrrolidine, from 0.005 to 16 μg/m^3. High levels of *N*-nitrosamines are present in leather tanning facilities with concentrations ranging from 0.05 to 10.8 μg/m^3.[5] The formation and occurrence of nitrosamines in the rubber industry depend on the production method and sampling area. *N*-Nitrosamines have been found in new car interiors,[14] tire retail shops, and tire storage areas.[15] The highest concentration of *N*-nitrosamines was found in the atmospheres where vulcanization and the associated post- treatment are performed. These elevated levels are the result of aminated vulcanization accelerators and nitrosating agents such as atmospheric nitrogen oxides. In 1988, Germany established a target value of 2.5 μg/m^3 total nitrosamines in workplaces.[12] Currently, no permissible exposure limits have been established by OSHA and the National Institute for Occupational Safety and Health (NIOSH) in the United States.[16,17]

Airborne *N*-nitrosamines are generally collected by trapping methods wherein a solution or solid sorbent is used in commercial air sampling cartridges. In some cases, contaminated air is passed through a 1 N KOH aqueous solution, and the analytes are extracted into an organic solvent and subsequently concentrated by solvent evaporation.[13] In other cases several hundreds of liters of air are pumped through a cartridge containing a solid sorbent to collect the sample. Cartridges are then transported to an analytical facility, and the collected nitrosamines are desorbed from the sorbent via a back flush with a mixture of dichloromethane and methanol.[18] Different nitrosamines are separated and detected using gas chromatography or high-performance liquid chromatography coupled to a thermal energy analyzer[5,6,10–13,18] or mass spectrometer.[15,19,20] Although these techniques can detect very low levels of nitrosamines, they are slow, expensive, and require sophisticated, expensive, and bulky instrumentation. Also, they are labor-intensive, and the remote analysis in an analytical facility prevents real-time monitoring of contamination levels. Considering these limitations in conventional air sampling and analysis, we have endeavored to create

inexpensive sensors for real-time distributed detection to minimize human exposure to *N*-nitrosamines.

Carbon nanotubes (CNTs)[21] are ideal for the formation of chemiresistive sensors[22–25] with electrical transport that is highly sensitive toward analyte binding.[26–31] CNT-based chemiresistive sensors are becoming increasingly important as they offer many advantages including low-power requirements, low-cost fabrication, real-time responses, and the capability to be miniaturized for portable deployment.[23] Motivated by these advantages, we have developed CNT chemiresistive sensors for the detection of *N*-nitrosamines.

The chemiresistive sensors reported herein are fabricated from single-walled carbon nanotubes (SWCNTs) functionalized by cobalt(III) tetraphenylporphyrin and can selectively detect *N*-nitrosamines in air at ppb levels. We found that the use of SWCNTs covalently functionalized by pyridyl groups provides superior sensitivity when compared to simple mixtures of cobalt(III) tetraphenylporphyrin and unfunctionalized CNTs. These simple devices are small, sensitive, selective, and operational at low power to enable portable sensing. We demonstrated that the materials can be readily integrated into a commercial sensing node, and the concentration of *N*-nitrosamines can be monitored remotely online using a computer or smartphone.

RESULTS AND DISCUSSION

The carcinogenic effect of *N*-nitrosamines is understood to involve the metabolic activation via heme-containing enzymes, cytochrome P450 2E1 and 2A6, primarily in the liver.[1] The oxidation of *N*-nitrosamines by P450 enzymes results in dealkylation to generate reactive alkyldiazohydroxides, which further decompose into diazonium ions that can irreversibly alkylate DNA.[1] Simple analysis of nitroamines suggests a strong contribution of a zwitterionic resonance structure, which should be conductive to coordination to metalloporphyrins. Indeed, stable and well-characterized *N*-nitrosamine metalloporphyrin complexes have been reported in the literature.[32–35]

To choose the optimal metalloporphyrin, we evaluated the chemiresistive responses of simple mixtures with CNTs to *N*-nitrosamines (Figure 1). NDMA, the most widely encountered environmental *N*-nitrosamine, was selected for sensor optimization and binding with metalloporphyrins. Chemiresistive sensors were fabricated by deposition of dispersed CNTs and a porphyrin selector sequentially onto the channel between two gold electrodes via solution drop casting. The SWCNTs we used in this initial screening contain a mixture of both metallic and semiconducting SWCNTs. During the sensing experiments (Figure S1), a 0.1 V bias was applied across the electrodes and the current was recorded. The response is given as a change in normalized conductance ($\Delta G/G_0$ (%) = $(I - I_0)/I_0 \times 100$, where I_0 is the initial current), and the three devices are averaged to give the sensor responses. All sensors comprising a metalloporphyrin and SWCNTs, control samples with a metal-free porphyrin, and selector-free SWCNTs exhibit a decrease in conductance upon 60 s of exposure to 100 ppm NDMA vapor (Figure 1, Figures S2–S3). The sensor experiments did not show significant variations between dry N_2 and air (2% RH) carrier gases. SWCNT sensors lacking porphyrins produced the smallest responses (~1%). The response increased upon

incorporating a porphyrin selector. Almost all of the metalloporphyrins produce higher responses than metal-free tetraphenylporphyrin (Htpp). Cobalt(III)

Having identified an optimal metalloporphyrin selector, we explored the use of different types of CNTs, including double- walled, few-walled, multiwalled, and (7,6)-chirality enriched ((7,6)-SWCNTs) carbon nanotubes. SWCNTs exhibited the best performance among the CNTs, with (7,6)-SWCNTs displaying the greatest performance (Figure 2a). The improved sensing response is attributed to the higher amount of semiconductive material in (7,6)-SWCNTs. In agreement with this finding, Ishihara et al. showed that semiconducting CNTs produce higher sensitivity relative to metallic CNTs in other chemiresistive sensors. The conductances of metallic CNTs are less perturbative to external stimuli as a result of the difficulty in quenching the metallic state.[36]

Covalent functionalization[37,38] can provide a robust connection between molecule and CNTs. A previous study demonstrated that covalent pyridyl functionalized SWCNTs[39] localized and electronically coupled iron porphyrins to CNTs for improved sensor performance.[31] As a result, we targeted 4-pyridyl functionalized (7,6)-SWCNTs with $Co(tpp)ClO_4$ for *N*-nitrosamine sensors. In accordance, we observed sensitivity enhancement from 11.9 ± 0.48 to 14.5 ± 0.18% using (7,6)- SWCNTs with a degree of functionalization of 1.9 pyridyl groups per 100 carbons and 16.8 ± 1.0% using a lower degree of functionalization of 1.4 pyridyl groups (Figure 2b). The observed lower response in the higher degree functionalized CNTs is attributed to the detrimental disruption of the CNT's π-electronic structure that localizes electronic states and scatters/traps carriers.

The cobalt(III) porphyrin functionalized 4-pyridyl (7,6)- SWCNT sensors were highly selective toward NDMA. Exposure of the devices to volatile organic compounds (VOCs) containing different functional groups, including hexane, toluene, water, acetone, ethyl acetate, tetrahydrofuran, ethanol, and acetonitrile, at twice the concentration of NDMA, 200 ppm, only showed very small responses (Figure 2c). A calibration curve of cobalt(III) porphyrin 4-pyridyl (7,6)- SWCNT sensors reveals a linear response at ppm levels of NDMA as shown in Figure 2d.

We hypothesized that the chemiresistive sensing mechanism of cobalt(III) porphyrin 4-pyridyl (7,6)-SWCNTs toward NDMA arises from the binding interaction between NDMA and cobalt(III) porphyrin. To verify this hypothesis, we carried out several spectroscopic studies to probe the binding of NDMA. Cobalt tetraphenylporphyrins display interesting magnetic properties in NMR studies. The parent metal-free tetraphenylporphyrin is diamagnetic, and its ^1H chemical shifts appear sharply on the NMR. Upon inserting cobalt(II) as the metal center, the complex becomes paramagnetic with broad and down-field shifted peaks as is common for NMR-active paramagnetic compounds. Oxidation of cobalt(II) to cobalt(III) increases the paramagnetic effects with peaks broadening to baseline levels (Figure S4). The sequential addition and binding of NDMA to cobalt(III) tetraphenylporphyrin complex create a strong ligand field to produce a low-spin d^6 diamagnetic state (Figure 3a).[40]

While ^{1}H NMR showed interesting binding and magnetic properties with the cobalt tetraphenylporphyrins, we further studied the binding of NDMA by UV–vis spectroscopy. Upon addition of increasing equivalents of NDMA to a solution of [Co(tpp)]ClO_4 in CH_2C_{l2}, we observe a shift of the Soret band of Co(tpp) from 310 to 330 nm (Figure 3b). Data fitting41 according to a 1:2 binding stoichiometry gave a binding constant (K_a) of 9.11 × 10^5 M^{-1} for this complex (Figure S5). The binding of NDMA to [Co(tpp)]ClO_4 was further confirmed by FTIR. NDMA has two characteristic IR peaks: ν_{NO} at 1460 cm^{-1} and ν_{NN} at 1035 cm^{-1}. Upon binding, the ν_{NO} peak shifts to a lower wavenumber, and the ν_{NN} shifts to a higher wavenumber; these shifts can be explained by a significant dipolar resonance contribution from NDMA (Figure 3c,d). This peak shifting results in the formation of overlapping ν_{NN} and ν_{NO} peaks at 1243 cm^{-1} (Figure 3c) and is consistent with other *N*-nitrosamine metalloporphyrin complexes.[32–34]

To detect environmentally relevant levels (ppb levels) of *N*-nitrosamines, we explored various device optimization parameters, including the relative amounts of selector to CNTs, device resistance range, and channel gap (Figure S7). Based on these studies, we converged on gold electrodes with a 300 μm channel gap with an active region 1 mm long and a resistance of 10–100 kΩ prepared by drop casting 0.5 μL of [Co(tpp)]ClO_4 in ODCB (1.0 mg/mL). Covalent functionalization usually increases the resistance of CNTs, which required a thicker sensing layer that is often used in order to achieve a targeted resistance range. The use of a relatively small channel gap was applied to minimize the layer thickness for more efficient penetration of gas molecules throughout the active sensing layer, thereby leading to higher sensitivity. The optimized device parameters allowed us to perform sensing at ppb levels of NDMA. Since cobalt(III) porphyrin-CNT sensors exhibit a linear increase in resistance within the concentrations and exposure times examined without a saturation level, we decided to utilize this feature for ppb-level NDMA detection. Using a longer 10 min exposure time, concentrations in the range of 1–1000 ppb can be readily detected in air. The calibration curve in the ppb concentration range exhibits a linear trend (Figure 4).

The effect of humidity on the response of cobalt(III) porphyrin-CNT sensors was examined. Experiments were conducted with 5 ppm NDMA under low to high relative humidity conditions (2 to 61%, Figure S8). No significant differences in response were observed across a range of humidity levels.

We also investigated the response of our cobalt(III) porphyrin-CNT sensors to other volatile *N*-nitrosamines including NDEA and NDBA. The sensors are responsive to both NDEA and NDBA with similar sensitivity (Figure S9). Concentrations as low as 1 ppb both nitrosamines are detectable in air. FTIR measurements confirm that NDEA and NDBA bind cobalt(III) porphyrin, with characteristic peaks between 1235 and 1258 cm^{-1} (Figure S6).

Chemiresistive sensors can be distributed at contamination sites for air monitoring, and this detection technology can provide communities and workers with actionable information regarding contamination levels and thereby help minimize exposure to harmful chemicals. As discussed earlier, conventional airborne *N*-nitrosamine detection cannot provide real-time and convenient on-site detection. We successfully integrated our cobalt(III) porphyrin-CNT sensors with a sensing chip, a piezoelectric pump that draws air into the sensing cartridge,

and a processor that controls the sensing node. It can be placed at any contamination site and has the advantage that the sensor's response can be read remotely using a computer or smartphone with Internet connection. Devices fabricated on glass slides can be inserted into the sensing cartridge of the sensing node. Exposure of the sensors to 10 min of 100 ppm NDMA in air gave a 0.54% response (Figure 5b). We attribute the difference in sensor responses as compared to those measured with a laboratory potentiostat to different electronic configurations between the sensing node and potentiostat. With a longer exposure time, 20 min, the commercial system gave a similar response (1.16%, Figure 5b) to potentiostat-based measurements (Figure 4).

CONCLUSIONS

In conclusion, we developed ultra-sensitive carbon nanotube based chemiresistive sensors for the detection of airborne *N*-nitrosamines. The sensors consist of covalent 4-pyridyl-(7,6)-SWCNTs functionalized with a cobalt (III) tetraphenylporphyrin selector. Mechanistic studies showed that the change in conductance is a result of the binding of *N*-nitrosamines to cobalt (III) tetraphenylporphyrin. These extremely sensitive sensors can detect 1 ppb of NDMA, NDEA, and NDBA. For distributed environmental air monitoring, we integrated the sensor devices with a commercial sensing node. Successful online detection of ppb levels of NDMA in air was readily feasible.

Supplementary Material

Refer to Web version on PubMed Central for supplementary material.

ACKNOWLEDGMENTS

This work was supported by the National Institute of Environmental Health Sciences Superfund Basic ResearchProgram, National Institute of Health, P42 ES027707. M.H. was supported by NIH Training Grant T32ES007020.

REFERENCES

(1). Yamazaki H; Inui Y; Yun C-H; Guengerich FP; Shimada T Cytochrome P450 2E1 and 2A6 Enzymes as Major Catalysts for Metabolic Activation of N-Nitrosodialkylamines and Tobacco-Related Nitrosamines in Human Liver Microsomes. Carcinogenesis 1992, 13, 1789–1794. [PubMed: 1423839]

(2). US EPA Technical Fact Sheet − N-Nitroso-Dimethylamine (NDMA); EPA United States Environmental Protection Agency, 2014.

(3). Dai N; Shah AD; Hu L; Plewa MJ; McKague B; Mitch WA Measurement of Nitrosamine and Nitramine Formation from NOx Reactions with Amines during Amine-Based Carbon Dioxide Capture for Postcombustion Carbon Sequestration. Environ. Sci. Technol 2012, 46, 9793–9801. [PubMed: 22831707]

(4). Dai N; Mitch WA Effects of Flue Gas Compositions on Nitrosamine and Nitramine Formation in Postcombustion CO2 Capture Systems. Environ. Sci. Technol 2014, 48, 7519–7526. [PubMed: 24918477]

(5). Safety OSHA and Health Information Bulletins: N-Nitroso Compounds in Industry; United States Department of Labor, 1990.

(6). Mahanama KRR; Daisey JM Volatile N-Nitrosamines in Environmental Tobacco Smoke: Sampling, Analysis, Emission Factors, and Indoor Air Exposures. Environ. Sci. Technol 1996, 30, 1477–1484.

(7). Mitch WA; Sedlak DL Formation of N-Nitrosodimethyl- amine (NDMA) from Dimethylamine during Chlorination. Environ. Sci. Technol 2002, 36, 588–595. [PubMed: 11878371]

(8). Scanlan RA; Barbour JF; Chappel CI A Survey of N- Nitrosodimethylamine in U.S. and Canadian Beers. J. Agric. Food Chem. 1990, 38, 442–443.

(9). MA Q; XI H-W; WANG C; BAI H; XI G-C; SU N; XU L-Y; WANG J-B Determination of Ten Volatile Nitrosamines in Cosmetics by Gas Chromatography Tandem Mass Spectrometry. Chin. J. Anal. Chem 2011, 39, 1201–1207.

(10). Mitch WA; Sharp JO; Trussell RR; Valentine RL; Alvarez-Cohen L; Sedlak DL N-Nitrosodimethylamine (NDMA) as a Drinking Water Contaminant: A Review. Environ. Eng. Sci 2003, 20, 389–404.

(11). Spiegelhalder B; Preussmann R Occupational Nitrosamine Exposure. 1. Rubber and Tyre Industry. Carcinogenesis 1983, 4, 1147–1152. [PubMed: 6883637]

(12). Oury B; Limasset JC; Protois JC Assessment of Exposure to Carcinogenic N-Nitrosamines in the Rubber Industry. Int. Arch. Occup. Environ. Health 1997, 70, 261–271. [PubMed: 9342627]

(13). Fajen J; Carson G; Rounbehler D; Fan T; Vita R; Goff U; Wolf M; Edwards G; Fine D; Reinhold V; et al. N- Nitrosamines in the Rubber and Tire Industry. Science 1979, 205, 1262–1264. [PubMed: 472741]

(14). Rounbehler DP; Reisch J; Fine DH Nitrosamines in New Motor-Cars. Food Cosmet. Toxicol 1980, 18, 147–151. [PubMed: 7390337]

(15). Marano RS; Updegrove WS; Machen RC Determination of Trace Levels of Nitrosamines in Air by Gas Chromatography/Low- Resolution Mass Spectrometry. Anal. Chem 1982, 54, 1947–1951. [PubMed: 7149262]

(16). Safety Occupational and Administration Health (OSHA) Chemical Sampling Information − N-Nitrosodimethylamine; United States Department of Labor.

(17). National Institute for Occupational Safety and Health (NIOSH) NIOSH Pocket Guide to Chemical Hazards: N-Nitro- sodimethylamine; Centers for Disease Control and Prevention.

(18). NIOSH Nitrosamines: Method 2522; NIOSH Manual of Analytical Methods, 1994, No. 2.

(19). Gough TA; Webb KS; Pringuer MA; Wood BJ A Comparison of Various Mass Spectrometric and a Chemiluminescent Method for the Estimation of Volatile Nitrosamines. J. Agric. Food Chem 1977, 25, 663–667. [PubMed: 858863]

(20). Webb KS; Gough TA; Carrick A; Hazelby D Mass Spectrometric and Chemiluminescent Detection of Picogram Amounts of N-Nitrosodimethylamine. Anal. Chem 1979, 51, 989–992.

(21). Schnorr JM; Swager TM Emerging Applications of Carbon Nanotubes. Chem. Mater 2011, 23, 646–657.

(22). Fennell JF Jr.; Liu SF; Azzarelli JM; Weis JG; Rochat S; Mirica KA; Ravnsbaek JB; Swager TM Nanowire Chemical/Biological Sensors: Status and a Roadmap for the Future. Angew. Chem., Int. Ed 2016, 55, 1266–1281.

(23). Schroeder V; Savagatrup S; He M; Lin S; Swager TM Carbon Nanotube Chemical Sensors. Chem. Rev 2019, 119, 599–663. [PubMed: 30226055]

(24). Kauffman DR; Star A Carbon Nanotube Gas and Vapor Sensors. Angew. Chem., Int. Ed 2008, 47, 6550–6570.

(25). Meyyappan M Carbon Nanotube-Based Chemical Sensors. Small 2016, 12, 2118–2129. [PubMed: 26959284]

(26). Paoletti C; He M; Salvo P; Melai B; Calisi N; Mannini M; Cortigiani B; Bellagambi FG; Swager TM; Di Francesco F; et al. Room Temperature Amine Sensors Enabled by Sidewall Functionalization of Single-Walled Carbon Nanotubes. RSC Adv. 2018, 8, 5578–5585. [PubMed: 30820317]

(27). Schnorr JM; van der Zwaag D; Walish JJ; Weizmann Y; Swager TM Sensory Arrays of Covalently Functionalized Single- Walled Carbon Nanotubes for Explosive Detection. Adv. Funct. Mater 2013, 23, 5285–5291.

(28). Dionisio M; Schnorr JM; Michaelis VK; Griffin RG; Swager TM; Dalcanale E Cavitand-Functionalized SWCNTs for N-Methylammonium Detection. J. Am. Chem. Soc 2012, 134, 6540–6543. [PubMed: 22475006]

(29). Weis JG; Ravnsbæk JB; Mirica KA; Swager TM Employing Halogen Bonding Interactions in Chemiresistive Gas Sensors. ACS Sens. 2016, 1, 115–119.

(30). Esser B; Schnorr JM; Swager TM Selective Detection of Ethylene Gas Using Carbon Nanotube-Based Devices: Utility in Determination of Fruit Ripeness. Angew. Chem., Int. Ed 2012, 51, 5752–5756.

(31). Savagatrup S; Schroeder V; He X; Lin S; He M; Yassine O; Salama KN; Zhang X-X; Swager TM Bio-Inspired Carbon Monoxide Sensors with Voltage-Activated Sensitivity. Angew. Chem., Int. Ed 2017, 56, 14066–14070.

(32). Chen L; Yi G-B; Wang L-S; Dharmawardana UR; Dart AC; Khan MA; Richter-Addo GB Synthesis, Characterization, and Molecular Structures of Diethylnitrosamine Metalloporphyrin Complexes of Iron, Ruthenium, and Osmium. Inorg. Chem 1998, 37, 4677–4688. [PubMed: 11670621]

(33). Xu N; Goodrich LE; Lehnert N; Powell DR; Richter-Addo GB Five- and Six-Coordinate Adducts of Nitrosamines with Ferric Porphyrins: Structural Models for the Type II Interactions of Nitrosamines with Ferric Cytochrome P450. Inorg. Chem 2010, 49, 4405–4419. [PubMed: 20392126]

(34). Yi GB; Khan MA; Richter-Addo GB The First Metalloporphyrin Nitrosamine Complex: Bis(Diethylnitrosamine)-(Meso-Tetraphenyl-Porphyrinato)Iron(III) Perchlorate. J. Am. Chem. Soc 1995, 117, 7850–7851.

(35). Richter-Addo GB Binding of Organic Nitroso Compounds to Metalloporphyrins. Acc. Chem. Res 1999, 32, 529–536.

(36). Ishihara S; O'Kelly CJ; Tanaka T; Kataura H; Labuta J; Shingaya Y; Nakayama T; Ohsawa T; Nakanishi T; Swager TM Metallic versus Semiconducting SWCNT Chemiresistors: A Case for Separated SWCNTs Wrapped by a Metallosupramolecular Polymer. ACS Appl. Mater. Interfaces 2017, 9, 38062–38067. [PubMed: 29022690]

(37). Karousis N; Tagmatarchis N; Tasis D Current Progress on the Chemical Modification of Carbon Nanotubes. Chem. Rev 2010, 110, 5366–5397. [PubMed: 20545303]

(38). Tasis D; Tagmatarchis N; Bianco A; Prato M Chemistry of Carbon Nanotubes. Chem. Rev 2006, 106, 1105–1136. [PubMed: 16522018]

(39). He M; Swager TM Covalent Functionalization of Carbon Nanomaterials with Iodonium Salts. Chem. Mater 2016, 28, 8542–8549.

(40). Sugimoto H; Ueda N; Mori M Preparation and Physicochemical Properties of Tervalent Cobalt Complexes of Porphyrins. Bull. Chem. Soc. Jpn 1981, 54, 3425–3432.

(41). Supramolecular; Http://Supramolecular.Org.

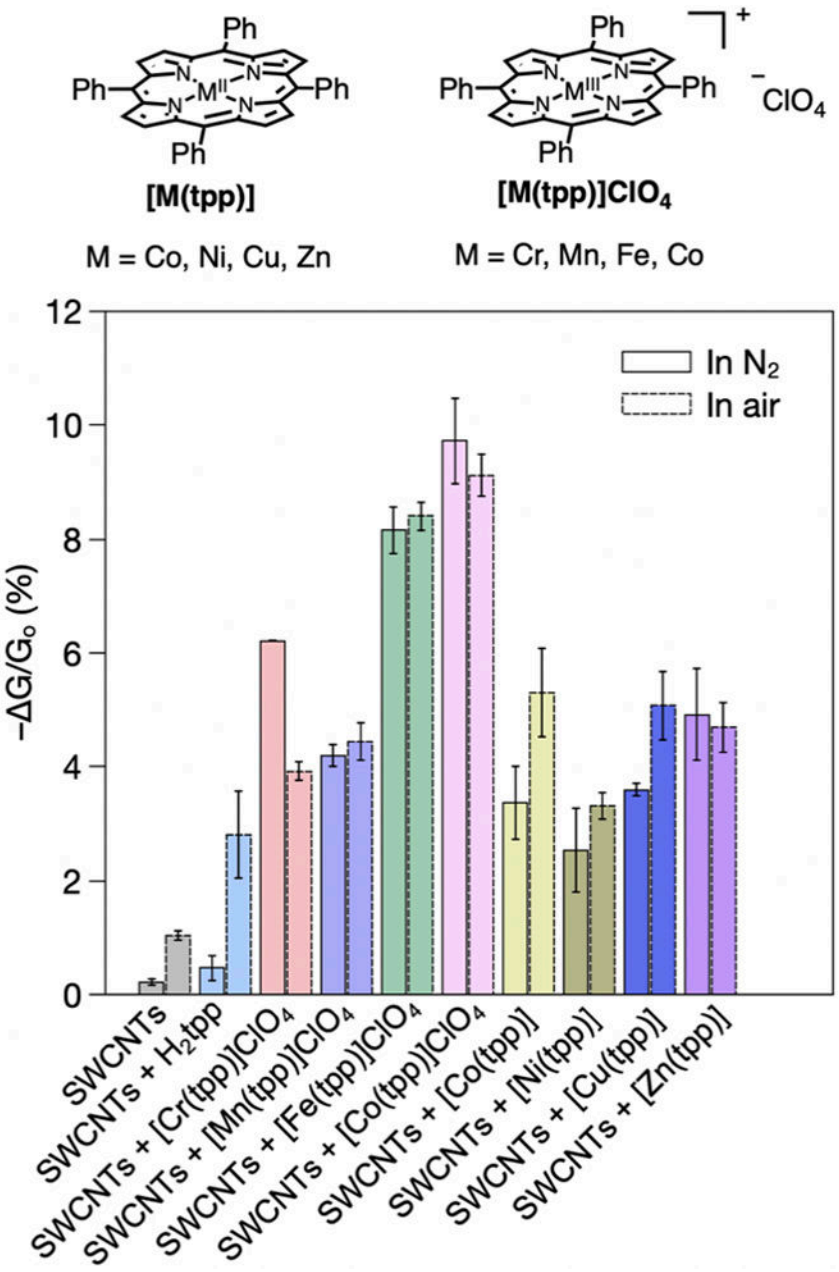

Figure 1.

Structure of metalloporphyrins (top). Response of different sensors comprise of metalloporphyrins and SWCNTs to 60 s exposure of 100 ppm NDMA in N_2 and air (bottom).

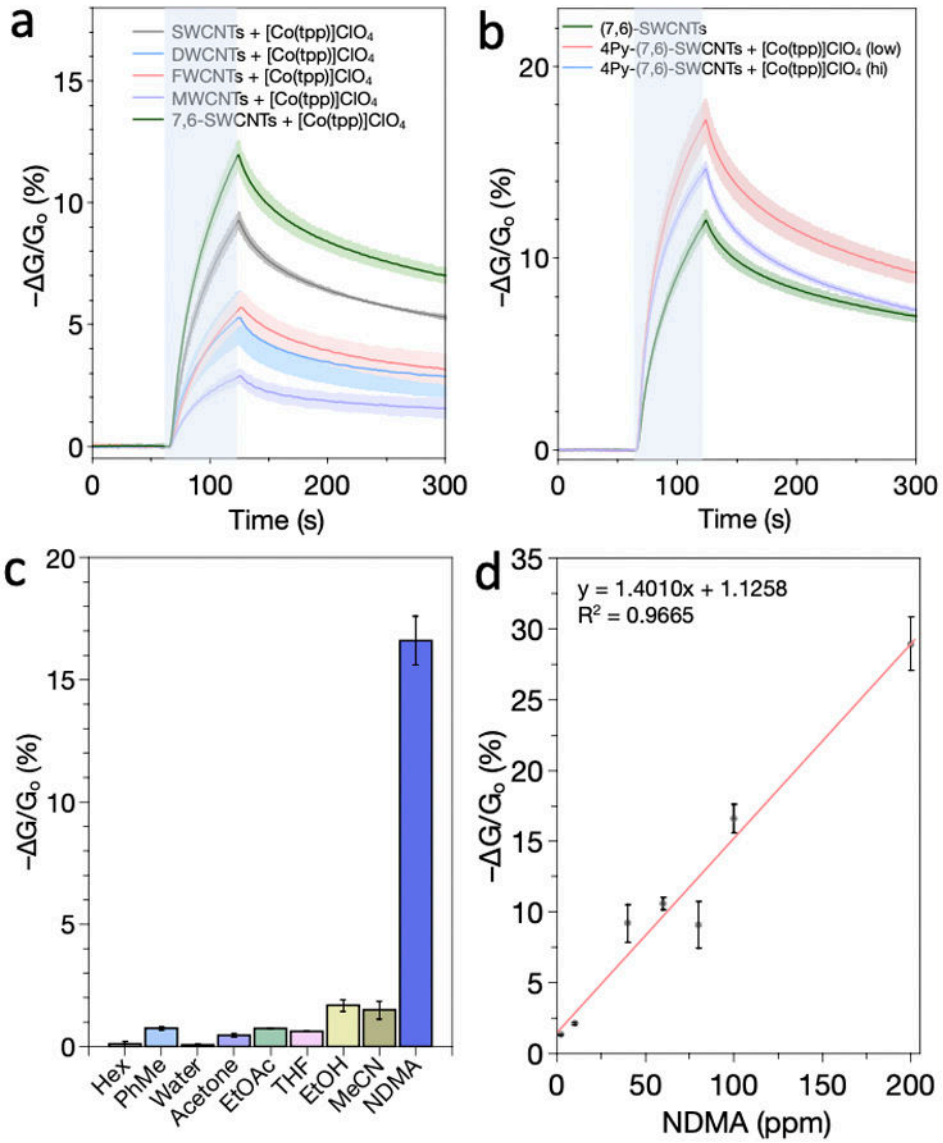

Figure 2.

Sensor optimization and selectivity. Three devices are averaged to give the sensor response. (a) Response of sensors fabricated with different types of CNTs with $[Co(tpp)]ClO_4$. (b) Improved sensor sensitivity using covalently functionalized 4-pyridyl (7,6)-SWCNTs with $[Co(tpp)]ClO_4$. (c) Response of 4-pyridyl (7,6)-SWCNTs with $[Co(tpp)]ClO_4$ towards different VOCs. (d) Calibration curve of 4-pyridyl (7,6)-SWCNTs with $[Co(tpp)]ClO_4$ at ppm concentrations. All sensing experiments were conducted in air with 60 s exposure to 100 ppm NDMA in (a) and (b), 100 ppm NDMA and 200 ppm VOCs in (c) and various concentrations in (d). Areas highlighted in light blue in (a) and (b) indicate exposure to NDMA.

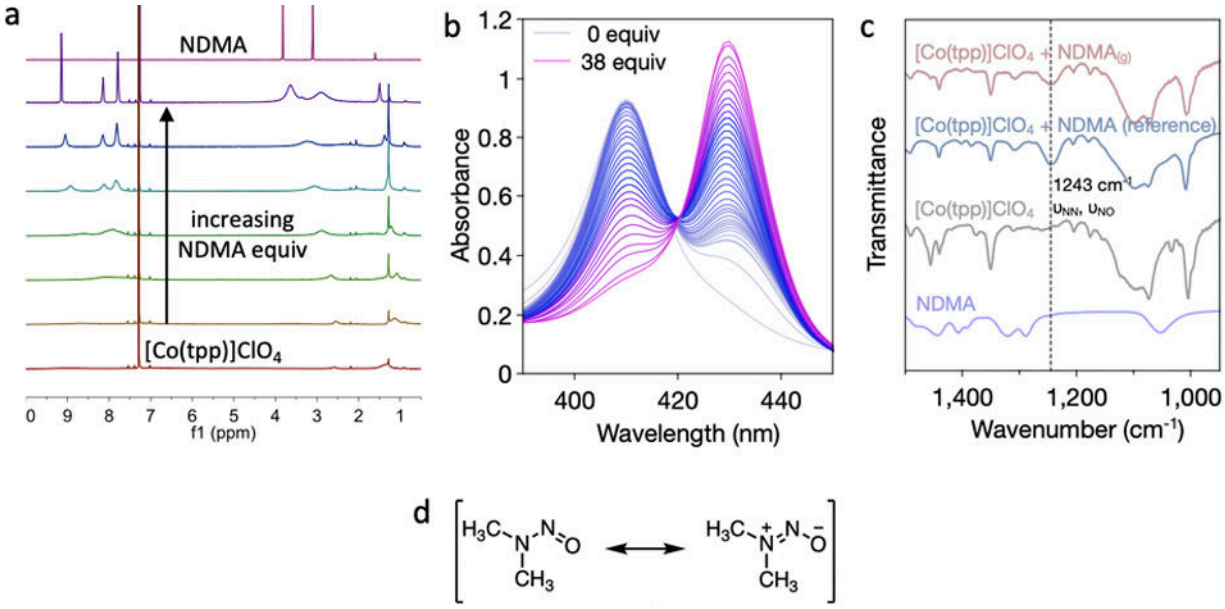

Figure 3.

(a) ^{1}H NMR of addition of increasing equivalents of NDMA to a solution of $[Co(tpp)]ClO_4$ in $CDCl_3$. (b) UV-Vis titration curve of NDMA to a solution of $[Co(tpp)]ClO_4$ in CH_2Cl_2. (c) FTIR of $[Co(tpp)]ClO_4$ and binding of NDMA to $[Co(tpp)]ClO_4$. d) Resonance structures of NDMA.

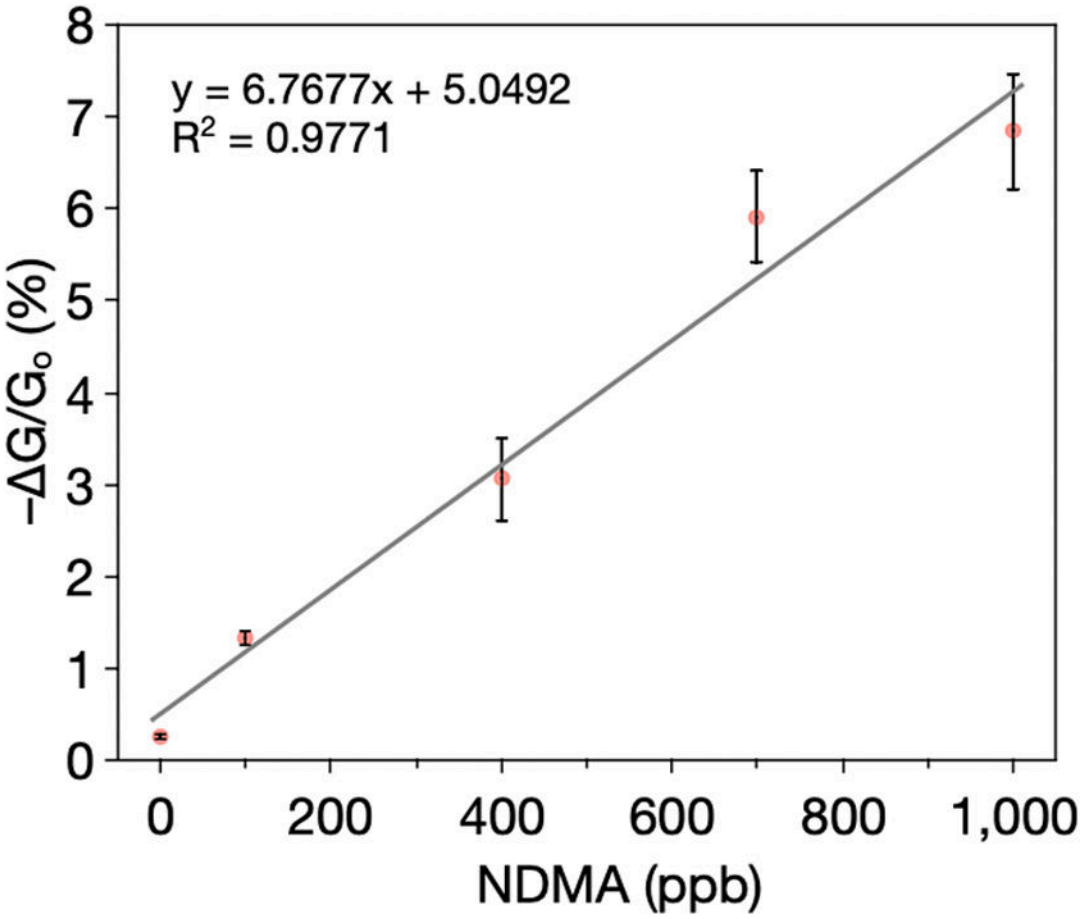

Figure 4.
Detection of NDMA in air at ppb levels.

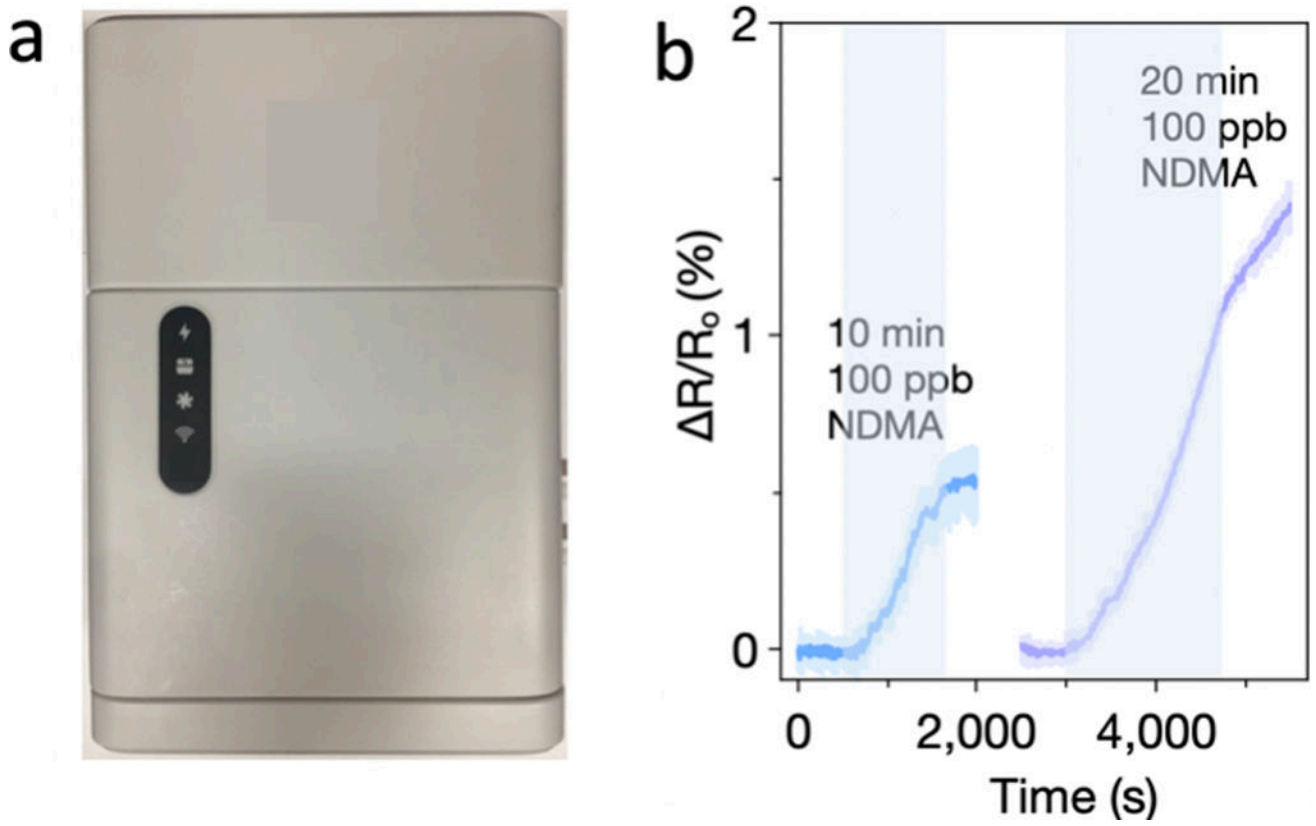

Figure 5.

(a) Commercial sensing node. (b) Sensing response to NDMA using a commercial sensing node. Areas highlighted in light blue indicate exposure to NDMA.